REVIEW ARTICLE

General Performance of Density Functionals

Sérgio Filipe Sousa, Pedro Alexandrino Fernandes, and Maria João Ramos*

REQUIMTE, Departamento de Química, Faculdade de Ciências, Universidade do Porto,
Rua do Campo Alegre, 687, 4169-007 Porto, Portugal

The density functional theory (DFT) foundations date from the 1920s with the work of Thomas and Fermi, but it was after the work of Hohenberg, Kohn, and Sham in the 1960s, and particularly with the appearance of the B3LYP functional in the early 1990s, that the widespread application of DFT has become a reality. DFT is less computationally demanding than other computational methods with a similar accuracy, being able to include electron correlation in the calculations at a fraction of time of post-Hartree−Fock methodologies. In this review we provide a brief outline of the density functional theory and of the historic development of the field, focusing later on the several types of density functionals currently available, and finishing with a detailed analysis of the performance of DFT across a wide range of chemical properties and system types, reviewed from the most recent benchmarking studies, which encompass several well-established density functionals together with the most recent efforts in the field. Globally, an overall picture of the level of performance of the plethora of currently available density functionals for each chemical property is drawn, with particular attention being dedicated to the relative performance of the popular B3LYP density functional.

Introduction

The density functional theory (DFT) has emerged during the past decades as a powerful methodology for the simulation of chemical systems. DFT is built around the premise that the energy of an electronic system can be defined in terms of its electron probability density, ρ. For a system comprising n electrons, $\rho(r)$ represents the total electron density at a particular point in space r. According to the DFT formalism, the electronic energy E is regarded as a functional of the electron density $E[\rho]$, in the sense that to a given function $\rho(r)$ corresponds a single energy, i.e., a one-to-one correspondence between the electron density of a system and its energy exists.

The advantage of DFT treatment over a more pure approach based on the notion of wavefunction can be best illustrated considering the following: for a system comprising n electrons, its wavefunction would have three coordinates for each electron and one more per electron if the spin is included, i.e., a total of $4n$ coordinates, whereas the electron density depends only on three coordinates, independently of the number of electrons that constitute the system.[1] Hence, while the complexity of the wavefunction increases with the number of electrons, the electron density maintains the same number of variables, independently of the system size.

Over time, many interesting reviews on DFT have been published.[2−11] These reviews have focused on a variety of aspects including the theory, methodological developments, and the practical application of DFT to specific problems. However, the computational development that has characterized the past

few years has dramatically enlarged the range of possibilities in the field. B3LYP has been for several years now the most widely used alternative, but nowadays a large number of density functionals at different levels of sophistification has become available. Despite this evolution, most users still continue to rely on the same density functionals they did 10 years ago. The present review tries to give an accurate account of the current status of the field, taking this progress into consideration, and including also the large number of benchmarking studies that have been published during the past 4 years, comparing the performance of several well-established density functionals with the most recent alternatives. The objective is hence 2-fold: (1) to illustrate the best level of performance that can be presently achieved with a density functional for each property and (2) to situate B3LYP in terms of performance for each given property among the plethora of existing functionals.

We start with a brief description of the historical development of the field, moving then to a presentation of the basic principles associated with this methodology, and highlighting the several types of density functionals currently available. Particular attention is dedicated to a detailed analysis of the performance of the currently available density functionals in the reproduction of a large variety of chemical properties, including bond lengths and angles, barrier heights, atomization energies, binding energies, ionization potentials, electron affinities, heats of formation, and several types of nonbonded interactions.

Basic Principles: The Hohenberg−Kohn Theorem

The concept of density functional emerged for the first time in the late 1920s, implicit in the work developed by E. Fermi[12]

* Corresponding author. E-mail: mjramos@fc.up.pt.

Sérgio Filipe Sousa finished his first degree in chemistry at the University of Porto, Portugal, in 2003, and has since then been pursuing a Ph.D. in theoretical chemistry at the Theoretical and Computational Chemistry Group of Professor M. J. Ramos, focusing mainly on the mechanistic study of Zn enzymes, with particular relevance to Farnesyltransferase.

Pedro Alexandrino Fernandes received his degree in chemistry at the University of Porto, Portugal. Afterward he obtained a Ph.D (2000) in molecular dynamics simulations of liquid interfaces and ion transfer, under the supervision of Prof. José Ferreira Gomes, in the same University. He has joined the University of Porto as an Associate Professor in 1999, and the research group of Prof. Maria João Ramos in 2000. Since then he has been dedicated to the field of computational biochemistry, in the areas of protein structure and dynamics, enzymatic catalysis and inhibition, and drug design.

Maria João Ramos completed her first degree in chemistry at the University of Porto, Portugal, her Ph.D. in muon research at The University, Glasgow, U.K., and a post-doc in molecular modeling at the University of Oxford, U.K. Back in Portugal since 1991, she is now a Professor at the University of Porto, the leader of a group working in computational biochemistry with three main lines of research: computational enzymatic catalysis, protein structure and dynamics, and drug design.

and L. H. Thomas,[13] which introduced the idea of expressing the energy of a system as a function of total electron density. In 1951, J. C. Slater[14] applied the very same basic idea into the development of the Hartree−Fock−Slater method, later known as Xα, initially regarded as an approximate methodology to the Hartree−Fock theory, but nowadays considered a predecessor theory of DFT.

Even though these theories were able to relate (albeit with several limitations) the energy and other properties of the system with the electron density, a formal proof of this notion came only in the 1960s, when P. Hohenberg and W. Kohn published a theorem[15] demonstrating that the ground-state energy of a nondegenerate electronic system and the correspondent electronic properties are uniquely defined by its electron density. However, although the Hohenberg−Kohn theorem confirms the existence of a functional relating the electron density and the energy of a system, it does not tell us the form of such functional. The search for functionals able to connect these two quantities remains one of the goals of DFT methods.

The Kohn−Sham Formalism

In 1965, W. Kohn and L. Sham[16] developed, with the introduction of atomic orbitals, a formalism that is the foundation for the current application of DFT in the computational chemistry field. This formalism yields a practical way to solve the Hohenberg−Kohn theorem for a set of interacting electrons, starting from a virtual system of noninteracting electrons having an overall ground-state density equal to the density to some real system of chemical interest where electrons do interact. The main problem behind initial DFT formalisms was the difficulty in representing the kinetic energy of the system. The central premise in the Kohn−Sham approach is that the kinetic energy functional of a system can be split into two parts: one part that can be calculated exactly and that considers electrons as noninteracting particles and a small correction term accounting for electron−electron interaction.

Following the Kohn−Sham formalism, within an orbital formulation, the electronic energy of the ground state of a system comprising n electrons and N nuclei can be written as

$$E[\rho] = -\frac{1}{2}\sum_{i=1}^{n}\int \Psi_i^*(r_1)\nabla_i^2\Psi_i(r_1)\,dr_1 - \sum_{X=1}^{N}\int\frac{Z_X}{r_{Xi}}\rho(r_1)\,dr_1 + \frac{1}{2}\int\int\frac{\rho(r_1)\,\rho(r_2)}{r_{12}}\,dr_1\,dr_2 + E^{XC}[\rho] \quad (1)$$

In eq 1, Ψ_i ($i = 1, 2, ..., n$) are the Kohn−Sham orbitals, the first term represents the kinetic energy of the noninteracting electrons, the second term accounts for the nuclear−electron interactions, and the third term corresponds to the Coulombic repulsions between the total charge distributions at r_1 and r_2. Finally, the fourth and last term, known as the exchange−correlation term, represents the correction to the kinetic energy arising from the interacting nature of the electrons, and all nonclassic corrections to the electron−electron repulsion energy. The biggest challenge of DFT is the description of this term.

The ground-state electron density $\rho(r)$ at a location r can be written as set of one-electron orbitals (the Kohn−Sham orbitals), given by

$$\rho(r) = \sum_{i=1}^{n}|\Psi_i(r)|^2 \quad (2)$$

The Kohn−Sham orbitals are determined by solving the Kohn−Sham equations. These can be derived by applying the variational principle to the electronic energy $E[\rho]$, with the charge density given by eq 2.

$$\hat{h}_i\Psi_i(r_1) = \epsilon_i\Psi_i(r_1) \quad (3)$$

In this equation $\hat{h}_i$ represents the Kohn−Sham Hamiltonian and ϵ_i is the Kohn−Sham orbital energy associated. The Kohn−Sham Hamiltonian can be written as

$$\hat{h}_i = -\frac{1}{2}\nabla_1^2 - \sum_{X=1}^{N}\frac{Z_X}{r_{Xi}} + \int\frac{\rho(r_2)}{r_{12}}\,dr_2 + V^{XC}(r_1) \quad (4)$$

In eq 4, V^{XC} is the functional derivative of the exchange−correlation energy, given by

$$V^{XC}[\rho] = \frac{\delta E^{XC}[\rho]}{\delta\rho} \quad (5)$$

Once E^{XC} is known, V^{XC} can be readily obtained. The importance of the Kohn−Sham orbitals is that they allow the density to be calculated from eq 2. The resolution of the Kohn−Sham equation is processed in a self-consistent fashion, starting from a tentative charge density ρ, which for a molecular system can be simply the result from the superposition of the atomic densities of the constituent atoms. An approximate form for the functional (which is fixed during all the iteration) that describes the dependence of the E^{XC} on the electron density is then used to calculate V^{XC}. This procedure allows the Kohn−Sham equations to be solved, yielding an initial set of Kohn−Sham orbitals. This set of orbitals is then used to calculate an improved density from eq 2. The entire process is repeated until the density and the exchange−correlation energy have satisfied a certain convergence criterion, previously chosen. At this point the electronic energy is calculated from eq 1.

The Kohn−Sham orbitals in each iteration are normally expressed in terms of a set of basis functions. In this sense, solving the Kohn−Sham equations corresponds to determining the coefficients in a linear combination of basis functions, in a

TABLE 1: Formal Scaling Behavior, as a Function of Basis Function N, of Various Electronic Structure Methods.

scaling behavior	method(s)
N^3	DFT
N^4	HF
N^5	MP2
N^6	MP3, CISD, CCSD, QCISD
N^7	MP4, CCSD(T), QCISD(T)
N^8	MP5, CISDT, CCSDT
N^9	MP6
N^{10}	MP7, CISDTQ, CCSDTQ

similar way to what is done in Hartree−Fock calculations. The choice of the basis set is therefore of great importance also in DFT calculations, but whereas in Hartree−Fock calculations the computational time associated scales as the fourth power of the number of basis functions, in DFT calculations it scales only as the third power (see Table 1).

The exchange−correlation energy E^{XC} is generally divided into two separate terms, an exchange term E^X and a correlation term E^C, although the legitimacy of such separation has been the subject of some doubt. The exchange term is normally associated with the interactions between electrons of the same spin, whereas the correlation term essentially represents those between electrons of opposite spin.

$$E^{XC}[\rho] = E^X[\rho] + E^C[\rho] \qquad (6)$$

These two terms into which E^{XC} can be decomposed (E^X and E^C) are themselves also functionals of the electron density. The corresponding functionals are known as the exchange functional and the correlation functional, respectively. Both components can be of two distinct types: local functionals, depending only on the electron density ρ, and gradient corrected, which depend on both ρ and its gradient $\Delta\rho$. These are reviewed over the next sections. Despite the progress in the field, it is important to retain that the main source of inaccuracy in DFT is normally a result of the approximate nature of the exchange−correlation functional.

Local Density Approximation

The local density approximation (LDA) constitutes the simplest approach to represent the exchange−correlation functional. In essence, LDA implicitly assumes that the exchange−correlation energy at any point in space is a function of the electron density at that point in space only and can be given by the electron density of a homogeneous electron gas of the same density.

The first local density approximation to the exchange energy was proposed by P. A. M. Dirac in 1930[17] and was used together with the Thomas−Fermi model,[12,13] in the so-called Thomas−Fermi−Dirac method.

$$E_{LDA}^{X,Dirac}[\rho] = -C_X \int \rho^{4/3}(r) \, dr \qquad (7)$$

where the constant C_X is given by

$$C_X = -\frac{3}{4} \cdot \left(\frac{3}{\pi}\right)^{1/3} \qquad (8)$$

Results were extremely modest. However, the inaccuracies verified were mainly due to the crude nature of the approximations considered for the kinetic energy functional in the initial Thomas−Fermi model, and not to the Dirac exchange functional itself. Large improvements were obtained with the Thomas−

Fermi−Dirac−Weizsäcker model,[18] which included gradient corrections to the Thomas−Fermi kinetic energy functional.

The local spin density approximation (LSDA), initially proposed by J. C. Slater,[14] represents a more general application of LDA, which introduces spin dependence into the functionals, solving several of the conceptual problems inherent to the early LDA approaches for systems that are subjected to an external magnetic field, systems that are polarized, and systems where relativistic effects are important. Within the LSDA approach, the exchange functional is given by

$$E_{LSDA}^X[\rho] = -2^{1/3} C_X \int (\rho_\alpha^{4/3} + \rho_\beta^{4/3}) \, dr \qquad (9)$$

In this equation α and β stand for spin up and spin down densities, respectively. For closed-shell systems, α and β are equal, and LSDA becomes virtually identical to LDA.

In LDA, the correlation energy E^C per particle is difficult to obtain separately from the exchange energy. This is normally achieved by using a suitable interpolation formula, starting from a set of values calculated for a number of different densities in a homogeneous electron gas. Several different formulations for this functional have been developed. One of such formulas is the one developed by S. Vosko, L. Wilk, and M. Nusair, known as Vosko−Wilk−Nusair or VWN,[19] which incorporated the Monte Carlo results of Ceperley[20] and of Ceperley and Alder.[21] Another popular correlation functional is the local correlation functional of Perdew (PL).[22]

Despite its conceptual simplicity, the LDA approximation is surprisingly accurate, notwithstanding some typical deficiencies, such as the inadequate cancellation of self-interaction contributions. In particular, LDA tends normally to underestimate atomic ground-state energies and ionization energies, whereas binding energies are typically overestimated. It is also known to overly favor high spin-state structures. LDA is in general worse for small molecules, improving with the size of the system. It is particularly suitable for systems having slowly varying densities, but surprisingly good results for several systems with relatively large density gradients have also been observed. A partial explanation for this success lies in the systematic cancellation of errors. In fact, LDA typically underestimates E^X but overestimates E^C resulting in unexpectedly good E^{XC} values.

Generalized Gradient Approximation Methods

Typical molecular systems are generally very different from a homogeneous electron gas. In fact, any real system is spatially inhomogeneous; i.e., it has a spatial varying density $\rho(r)$. Generalized gradient approximation methods (GGAs) take into account this effect, by making the exchange and correlation energies dependent not only on the density but also on the gradient of the density $\Delta\rho(r)$.

The development of GGA methods, sometimes also credited as nonlocal methods, has followed two main lines. The first one, of more empirical nature and initially proposed by Becke,[23−28] is based on numerical fitting procedures involving large molecular training sets. Exchange functionals that follow this philosophy include Becke88 (B),[29] Perdew−Wang (PW),[30] modified-Perdew−Wang (mPW),[30,31] OptX (O),[32] and X.[33] Typically, these functionals render particularly accurate atomization energies and reaction barriers for molecules.[23,24] However, this level of success is not observed in solid-state physics, with several important properties being poorly described.[34] The second group of GGA methods, advocated by Perdew[30,34−41] and more rational-based, considers that the development of exchange−correlation functionals should be anchored in basic

10442 *J. Phys. Chem. A, Vol. 111, No. 42, 2007*

Sousa et al.

principles derived from quantum mechanics, including scaling relations, correct limits for high and low densities, correct LSDA limit for slowly varying densities, and the fulfillment of exact relations on the exchange and correlation holes. Among the exchange functionals based on this principle are Becke86 (B86),[23] Perdew 86 (P),[37] Perdew−Burke−Ernzerhof (PBE),[40] and modified-Perdew−Burke−Ernzerhof (mPBE).[40,42] These functionals normally have some problems in competing with the fitted functionals for the determination of atomization energies and reaction barriers for molecular reactions but are actually better in predicting solid-state properties.[25,34]

For the correlation functional, several different formulations have been developed. Examples of GGA correlation functionals include Becke 88 (B88),[43] Perdew 86,[37] Perdew−Wang 91 (PW91),[38] and the extremely popular Lee−Yang−Parr (LYP),[44] which is constructed from the Colle−Salvetti correlation energy formula.[45]

In general, GGA methods represent a significant improvement over the local methods. In fact, GGA methods tend to give better total energies,[46] atomization energies,[29,46,47] structural energy differences, and energy barriers.[24,48] GGA methods tend to expand and soften bonds,[47] compensating for the LDA tendency to overbind.[40] However, the accuracy of GGA methods is still not enough for a correct description of many chemical aspects of molecules. For example, although GGA methods normally give reliable results for covalent, ionic, metallic, and hydrogen bridge bonds, they typically fail for van der Waals interactions.[49,50] In the case of the solid state, GGA functionals do not yield significantly better results than LDA,[51−57] nor in the calculation of ionization potentials and electron affinities.[47,58] Furthermore, the differences obtained when using different GGAs are often almost as large as those between individual GGAs and LDA functionals.

More recently, a new class of very promising DFT functionals based on the GGA was developed by including additional semi-local information beyond the first-order density gradient contained in the GGAs. These methods, termed meta-GGA (M-GGA), depend explicitly on higher order density gradients, or typically on the kinetic energy density, which involves derivatives of the occupied Kohn−Sham orbitals. These methods represent a significant improvement in the determination of properties such as atomization energies. However, they are more technically challenging, with several difficulties in terms of numerical stability. Several M-GGA functionals for the exchange functional, correlation functional or both have been developed. Examples include B95,[27] KCIS,[59] TPSS,[60] and VSXC.[61]

Hybrid Density Functional Methods

Hybrid density functional (H-GGA) methods combine the exchange−correlation of a conventional GGA method with a percentage of Hartree−Fock (or exact) exchange. A certain degree of empiricism is used in optimizing the weight factor for each component and the functionals that are mixed. In fact, the exact amount of Hartree−Fock exchange cannot be assigned from first-principles and therefore is fitted semiempirically. One way to do so is to fit these coefficients to experimental atomization energies, ionization potentials, proton affinities, total atomic energies, and other data, for a representative set of small molecules.[62]

Hybrid functionals have allowed a significant improvement over GGAs for many molecular properties. For this, they have become a very popular choice in quantum chemistry and are now widely used. However, in solid-state physics this type of

functional was much less successful due to difficulties in computing the exact-exchange part within a plane-wave basis set. Examples of hybrid density functionals include B3LYP,[27,29,44] B3P86,[27,29,37] B3PW91,[27,29,38] B97-1,[63] B97-2,[63] B98,[64] BH&HLYP,[29,44] MPW1K,[31,38,65,66] mPW3LYP,[31,38,44] O3LYP,[44,67] and X3LYP.[29,33,39,44]

Hybrid-meta GGA methods (HM-GGA) represent a new class of density functionals, based on a similar concept to the M-GGA functionals, and under active development. The difference lies in the fact that they start from M-GGAs instead of standard GGAs. Hence, these methods depend on the Hartree−Fock exchange, the electron density and its gradient, and the kinetic energy density. Examples of HM-GGA[31,38,59,68] exchange−correlation functionals include B1B95,[27,29] BB1K,[27,29,69] MPW1B95,[27,31,38,70] MPW1KCIS,[31,38,59,68] PBE1KCIS,[40,59,71] TPSS1KCIS,[59,60,72] and TPSSh.[60] These methods represent an improvement over the previous formalisms, particularly in the determination of barrier heights and atomization energies.

Most Common DFT Functionals

Table 2 gives an overview of some of the most common density functionals, with the indication of the type of functional and of the correspondent exchange and correlation functionals. This table lists also the current quantum chemical programs that include each of these density functionals by default in their currently distributed version. It should be noted, however, that many of these programs are highly flexible and permit the user to construct new density functionals by using any mixture of one or more exchange functionals, one or more correlation functionals, and any amount of Hartree−Fock exchange. In addition, there is not a standard naming convention, although generally the most popular density functionals have the same name in the several software programs. The reader should also be aware that in some cases the implementation of a given density functional may vary slightly from program to program. For all these reasons this list should be regarded only as a first indicator on the density functionals included on each program.

Figure 1 presents an estimate of uses of the several density functionals presented in Table 2, based on the number of occurrences of their names in the journal titles and abstracts analyzed from the ISI Web of Science (2007). B3LYP is by far the most popular density functional in chemistry, representing 80% of the total of occurrences of density functionals in the literature, in the period 1990−2006. Despite the progress in the field, and the appearance of several new functionals every year, B3LYP continues to dominate the field, maintaining a percentage of 81−84% throughout the past 5 years. Other popular density functionals are BLYP (5%), B3PW91 (4%), BP86 (3%), and B3P86 (2%).

General Performance of Density Functionals

"Jacob left Beer-Sheba and went toward Haran. He came to a certain place and stayed there for the night, because the sun had set. Taking one of the stones of the place, he put it under his head and lay down in that place. And he dreamed that there was a ladder set up on the earth, the top of it reaching to heaven; and the angels of God were ascending and descending on it." (Genesis 28.10−12)

The number and sophistication of available density functionals is rapidly increasing. In June 2000, J. Perdew presented at the DFT2000 symposium in Menton, France, his vision regarding the progress in the field in the form of Jacob's Ladder,[82] containing five different rungs, comprising five generations of DFT functionals (see Figure 2). In Perdew's vision of Jacob's

**TABLE 2: Summary of the Most Common Density Functional Theory Functionals, with the Indication of the Current Quantum Chemical Programs That Include These Functionals**[a]

functionals	year	type	χ	exchange functional	correlation functional	ref	ADF v. 2006.01	GAMESS UK v. 7.0	Gaussian v. 03	Jaguar v. 7.0	Molpro v. 2006.1	NWChem v. 5.0	Turbomole v. 5.9.1
									quantum chemical programs				
B1B95	1996	HM-GGA	25	Becke88	Becke95	27, 29	−	√	√	√	√	−	−
B3LYP	1994	H-GGA	20	Becke88	Lee−Yang−Parr	27, 29, 44	√	√	√	√	√	√	√
B3P86	1993	H-GGA	20	Becke88	Perdew86	27, 29, 37	−	√	√	√	−	−	−
B3PW91	1993	H-GGA	20	Becke88	Perdew−Wang91	27, 29, 38	−	√	√	√	−	−	−
B97-1	1998	H-GGA	21	B97-1	B97-1	63	√	√	√	√	√	√	−
B97-2	2001	H-GGA	21	B97-2	B97-2	63	√	√	√	−	−	√	−
B97-3	2005	H-GGA	26.93	B97-2	B97-3	63, 73	−	√	−	−	−	√	−
B98	1998	H-GGA	21.98	B98	B98	64	−	−	√	√	−	√	−
BB1K	2004	HM-GGA	42	Becke88	Becke95	27, 29, 69	−	√	−	√	−	√	−
BB95	1996	M-GGA	0	Becke88	Becke95	27, 29	−	√	√	√	√	−	−
BH&HLYP	1993	H-GGA	50	Becke88	Lee−Yang−Parr	29, 44	√	−	√	√	−	√	√
BLYP	1988	GGA	0	Becke88	Lee−Yang−Parr	29, 44	√	√	√	√	√	√	√
BMK	2004	HM-GGA	42	BMK	BMK	74	−	−	−	−	−	−	−
BP86	1988	GGA	0	Becke88	Perdew86	29, 37	√	√	√	√	√	√	√
BPBE	1996	GGA	0	Becke88	Perdew−Burke−Ernzerhof	29, 40	√	√	√	√	√	√	−
BPW91	1991	GGA	0	Becke88	Perdew−Wang91	29, 38	√	√	√	√	√	√	−
G96LYP	1996	GGA	0	Gill96	Lee−Yang−Parr	44, 75	−	−	√	−	−	−	−
G96HLYP	2005	GGSC	0	Gill96	half-Lee−Yang−Parr	44, 67, 75	−	−	−	−	−	−	−
HCTH	1998	GGA	0	Hamprecht−Cohen−Tozer−Handy	Hamprecht−Cohen−Tozer−Handy	63	√	√	√	√	√	−	−
M05	2005	HM-GGA	28	M05	M05	76	−	−	−	√	−	√	−
M05-2X	2005	HM-GGA	56	M05-2X	M05-2X	77	−	−	−	√	−	√	−
MOHLYP	2005	GGSC	0	metal-adjusted OptX	half-Lee−Yang−Parr	44, 67	−	−	−	−	−	−	−
MPW1B95	2004	HM-GGA	31	modified Perdew−Wang91	Becke95	27, 31, 38, 70	−	−	−	−	−	√	−
MPW1K	2000	H-GGA	42.8	modified Perdew−Wang91	Perdew−Wang91	31, 38, 65, 66	√	−	−	√	−	√	−
MPW3LYP	2004	H-GGA	21.8	modified Perdew−Wang91	Lee−Yang−Parr	31, 38, 44	−	−	−	√	−	−	−
MPWB1K	2004	HM-GGA	44	modified Perdew−Wang91	Becke95	27, 31, 38, 78	−	−	−	√	−	√	−
mPWB95	1998	M-GGA	0	modified Perdew−Wang91	Becke95	27, 31, 38	−	√	−	−	−	−	−
MPW1KCIS	2004	HM-GGA	15	modified Perdew−Wang91	Krieger−Chen−Iafrate−Savin	31, 38, 59, 68	−	−	−	−	−	−	−
mPWKCIS	2004	M-GGA	0	modified Perdew−Wang91	Krieger−Chen−Iafrate−Savin	31, 38, 59	√	−	√	−	−	−	−
MPWKCIS1K	2004	HM-GGA	41	modified Perdew−Wang91	Krieger−Chen−Iafrate−Savin	31, 38, 59, 68	−	−	−	−	−	−	−
mPWLYP	1998	GGA	0	modified Perdew−Wang91	Lee−Yang−Parr	31, 38, 44	√	−	√	√	−	√	−
mPWPW91	1998	GGA	0	modified Perdew−Wang91	Perdew−Wang91	31, 38	√	−	√	√	−	√	−
O3LYP	2001	H-GGA	11.61	OptX	Lee−Yang−Parr	32, 44, 79	√	−	√	−	−	−	−
OLYP	2001	GGA	0	OptX	Lee−Yang−Parr	32, 44	√	−	√	−	−	√	−
PBE	1996	GGA	0	Perdew−Burke−Ernzerhof	Perdew−Burke−Ernzerhof	40	√	√	√	√	√	√	√
PBE1PBE	1996	H-GGA	25	Perdew−Burke−Ernzerhof	Perdew−Burke−Ernzerhof	40	√	−	√	√	√	√	√
PBE1KCIS	2005	HM-GGA	22	Perdew−Burke−Ernzerhof	Krieger−Chen−Iafrate−Savin	40, 59, 71	−	−	−	−	−	−	−
PBEKCIS	2004	M-GGA	0	Perdew−Burke−Ernzerhof	Krieger−Chen−Iafrate−Savin	40, 59	√	−	√	−	−	−	−
PW6B95	2005	HM-GGA	28	PW6B95	PW6B95	80	−	−	−	√	−	√	−
PWB6K	2005	HM-GGA	46	PWB6K	PWB6K	80	−	−	−	√	−	√	−
SPWL	1992	LSDA	0	Slater	Perdew−Wang local	39, 81	−	√	−	−	−	−	−
SVWN3	1981	LSDA	0	Slater	VWN no. 3	19, 81	−	−	√	√	√	√	√
SVWN5	1981	LSDA	0	Slater	VWN no. 5	19, 81	√	√	√	√	√	√	√
TPSS	2003	M-GGA	0	Tao−Perdew−Staroverov−Scuseria	Tao−Perdew−Staroverov−Scuseria	60	√	−	−	−	−	√	√
TPSS1KCIS	2004	HM-GGA	13	Tao−Perdew−Staroverov−Scuseria	Krieger−Chen−Iafrate−Savin	59, 60, 72	−	−	−	−	−	−	−
TPSSh	2003	HM-GGA	10	Tao−Perdew−Staroverov−Scuseria	Tao−Perdew−Staroverov−Scuseria	60	√	−	−	−	−	√	√
TPSSKCIS	2004	M-GGA	0	Tao−Perdew−Staroverov−Scuseria	Krieger−Chen−Iafrate−Savin	59, 60	√	−	√	−	−	−	−
TPSSPWL	2004	GGE	0	Tao−Perdew−Staroverov−Scuseria	Perdew−Wang local	39, 60	−	−	−	−	−	−	−
TPSSVWN5	2004	GGE	0	Tao−Perdew−Staroverov−Scuseria	VWN no. 5	19, 60	−	−	√	−	−	√	−
VSXC	1998	M-GGA	0	Van Voorhis−Scuseria	Van Voorhis−Scuseria	61	√	−	√	−	√	−	−
X3LYP	2004	H-GGA	21.8	Becke88 + Perdew−Wang91	Lee−Yang−Parr	29, 33, 39, 44	√	−	−	√	−	−	−
XLYP	2004	GGA	0	Becke88 + Perdew−Wang91	Lee−Yang−Parr	29, 33, 39, 44	√	−	−	√	−	−	−

[a] χ, percentage of HF exchange in the functional; LDA, local density approximation; GGA, generalized gradient approximation; GGSC, generalized gradient with scaled correction; M-GGA, meta generalized gradient approximation; H-GGA, hybrid generalized gradient approximation; HM-GGA, hybrid meta generalized gradient approximation.
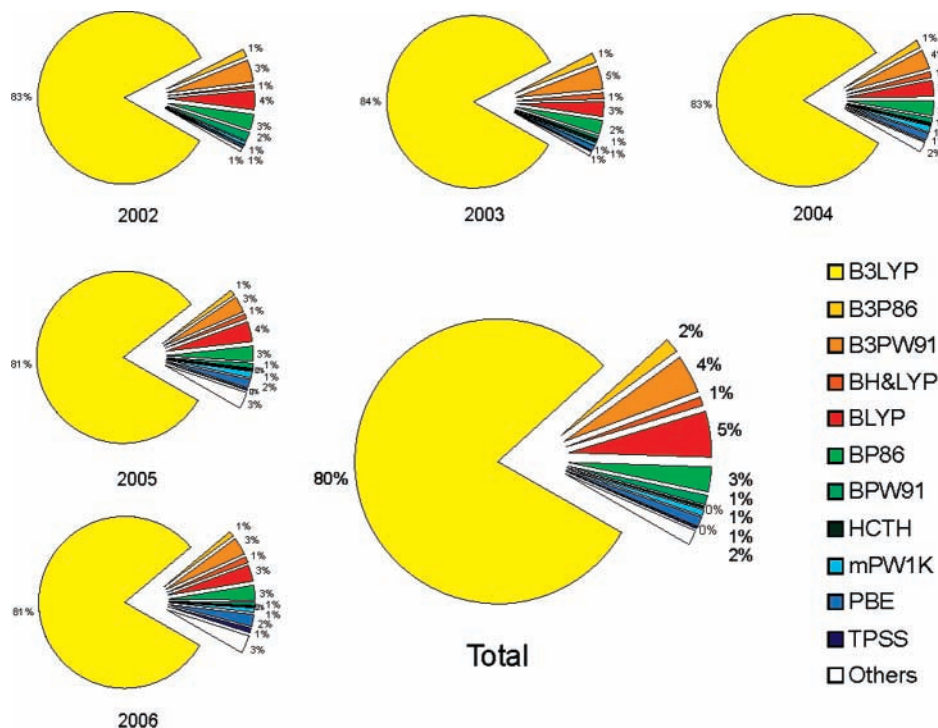
Figure 1. Percentage of occurrences of the names of the several functionals indicated in Table 2, in journal titles and abstracts, analyzed from the ISI Web of Science (2007).
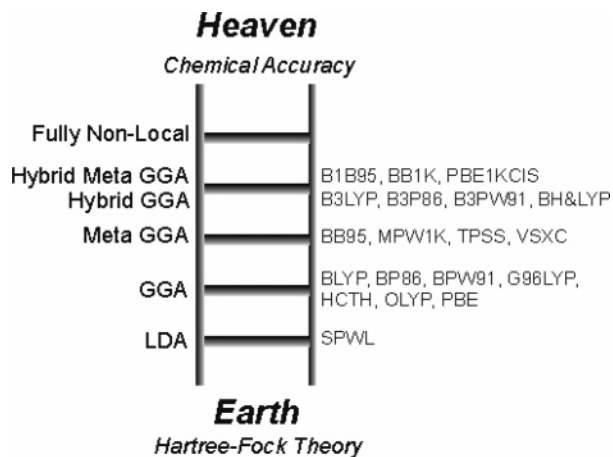
Figure 2. Jacob's ladder for the five generation of DFT functionals, according to the vision of J. Perdew,[82] with indication of some of the most common DFT functionals within each rung.

ladder, the users take the place of the angels, climbing or descending the ladder, according to their needs for precision or computational efficiency. Figure 2 represents Jacob's ladder, as proposed by J. Perdew, with the five rungs representing the hierarchy of density approximations: the local density approximation or LDA (first rung), the generalized gradient approximation or GGA (second rung), the meta generalized gradient approximation M-GGA (third rung), the hybrid generalized gradient approximation (or H-GGA) and the hybrid meta generalized gradient approximation (or MH-GGA) (fourth rung), and finally the fully nonlocal description (the fifth rung). Within this view, each rung adds something more to the design elements of the lower rungs, while retaining their gist. Although each rung has particular strengths and weaknesses, as outlined in the preceding sections, the global outcome for most properties is a steady improvement in the quality of the results and an increase in the computational cost associated, when moving from the lower to the higher rungs.

Technical sophistication and effective accuracy do not necessarily walk hand in hand. Although the performance of HM-GGA and H-GGA methods is traditionally better than GGAs, and particularly better than LDA methods, results vary from functional to functional. Furthermore, the performance of each functional is not uniform, depending on the property under evaluation, and on the type of system under study. The number of density functionals currently available is high and ever increasing. In particular, the past few years have been fertile in new density functionals. The performance of a large number of DFT functionals has been recently evaluated across a wide range of problem types. A comprehensive overview of the benchmarking studies published during the past 4 years, comprising a total of 57 comparisons of different density functionals in the calculation of several properties of chemical interest against experimental data or very high-level computational results, is presented below, together with the relative performance of B3LYP in each study, trying to provide a broad coverage of the remarkable development that has characterized the past few years of this field of research, and of its current state. A summary of these comparisons is presented in Table 3. Less recent comparisons of the performance of density functionals, significantly more limited in the number and novelty of the functionals tested, can be found elsewhere; examples include the calculation of molecular geometries and vibrational properties,[83-88] barrier heights,[65,89] electron affinities, ionization potentials and heats of formation,[90-96] hydrogen-bonding energies,[97-103] and conformational energies.[104]

Structure. *Bond Lengths.* The performance of the various density functionals is usually quite good in the prediction of minimum energy structures. The density functionals B3LYP, B3PW91, B3P86, BLYP, BPW91, and BP86 have been evaluated with eight different basis sets in the description of the molecular geometries for a set of 17 first-row closed-shell molecules of interest in atmospheric chemistry by Wang and Wilson.[105] The test set considered comprised a total of 26 experimentally determined bond lengths. In this study, the lowest

TABLE 3: Summary of the Benchmarking Studies on Density Functionals Published during the Last 4 Years, with Major Emphasis Being Given to Performance of B3LYP and Its Ranking among the Density Functionals Tested, and to the Best Functional for Each Property in Each Study

	B3LYP MUE	B3LYP ranking	best results functional (MUE)	dataset size	dataset characteristics	av. value in the dataset[a]	basis set	ref
				Structure				
A. bond lengths (Å)	0.008	3/6	BPW91 (0.007)	26 bond lengths	17 first-row closed shell molecules	1.493	Aug-cc-PV5Z	105
	0.06	12/12	MPW1K (0.01)	10 bond lengths	5 saddle-point geometries of H-transfer reactions	1.17	MG3S	70
	0.008	1/5	B3LYP (0.008)	44 bond lengths	32 first-row closed shell molecules	1.186	6-311+G**	106
	0.014	5/42	MPW3LYP (0.013)	13 bond lengths	13 metal compounds	1.689	DZQ/TZQ	67
	0.16	27/42	SVWN3 (0.05)	8 bond lengths	8 metal compounds	2.11	DZQ/TZQ	107
	0.007	2/37	VSXC (0.006)	71 bond lengths	44 small organic molecules	n/a	Aug-cc-pVQZ	108
B. angles (deg)	0.75	1/6	B3LYP (0.75)	10 bond angles	10 first-row closed shell molecules	108.99	Aug-cc-pV5Z	105
	1.94	5/6	c-SVWNV (1.82)	16 bond angles	12 first-row closed shell molecules	110.67	6-311+G**	106
	1.20	11/37	PBE1PBE (1.11)	34 bond angles	27 small organic molecules	n/a	Aug-cc-pVQZ	108
C. H bonds (Å)	0.02	7/15	MPW3LYP (0.01)	4 distances	4 H-bonding dimers	2.81	MG3S	70
D. weak interactions (Å)	1.02	15/15	B97-1 (0.08)	4 distances	4 rare-gas dimers	3.27	MG3S	70
				Kinetics (kcal/mol)				
A. barrier heights	4.7	11/22	MPW1K (1.4)	6 barrier heights	representative dataset of 6 H-transfer reactions	11.85	MG3S	109
	4.31	14/15	BB1K (1.16)	42 barrier heights	mostly open-shell H-transfer reactions	13.96	MG3S	70
	3.04	15/25	BB1K (1.50)	76 barrier heights	38 H-transfer reactions + 38 non-H-transfer reactions	18.12	MG3S	80
	4.73	17/42	BB1K (1.14)	6 barrier heights	A representative dataset of 6 H-transfer reactions	11.85	MG3S	107
	4.50	17/29	BB1K (1.37)	76 barrier heights	38 H-transfer reactions + 38 non-H-transfer reactions	18.12	MG3S	68
	4.30	7/37	BB1K (1.05)	23 barrier heights	23 small radical transition-state reactions	12.29	Aug-cc-pVTZ	108
	3.10	2/37	B1LYP (2.58)	6 barrier heights	6 large singlet transition-state reactions	27.55	Aug-cc-pVTZ	108
				Thermochemistry (kcal/mol)				
A. atomization energies	2.19	1/6	B3LYP (2.19)	17 compounds	17 first-row closed shell molecules	270.15	Aug-cc-pV5Z	105
	0.7	5/22	VSXC (0.5)	6 compounds	6 organic molecules	517.22	MG3S	109
	0.90	9/15	X1B95 (0.52)	109 compounds	109 organic and inorganic molecules	497.65	MG3S	70
	0.91	12/25	PW6B95 (0.40)	109 compounds	109 organic and inorganic molecules	497.65	MG3S	80
	0.61	4/42	MPW3LYP (0.43)	6 compounds	6 organic molecules	517.22	MG3S	107
	16.7	29/42	BLYP (5.3)	9 compounds	9 metal dimers	56.8	DZQ/TZQ	107
	26.3	27/42	BLYP (5.8)	9 compounds	9 metal dimers	56.8	DZQ/TZQ	67
B. binding energies	6.5	10/42	TPSS1KCIS (5.4)	21 compounds	21 transition metals	82.7	DZQ/TZQ	67
	12.0	7/7	M05 (7.8)	18 compounds	18 transition metals	65.5	QZVP	110
C. ionization potentials	4.72	14/15	MPWB1K (2.05)	13 compounds	6 atoms and 7 molecules	253.84	MG3S	70
	4.72	18/25	MPWB1K (2.05)	13 compounds	6 atoms and 7 molecules	253.84	MG3S	80
	3.8	1/6	B3LYP (3.8)	88 compounds	88 atoms and molecules from the G3 test set	253.13	6-311+G**	106
	7.2	27/42	OLYP (3.1)	7 compounds	7 atoms (including 5 metals)	202.6	DZQ/TZQ	67
	5.1	13/37	B1B95 (4.25)	37 compounds	derived from the Gaussian G2/97 test set	n/a	Aug-cc-pVTZ	108
D. electron affinities	2.29	4/15	B98 (1.84)	13 compounds	6 atoms and 7 molecules	38.16	MG3S	70
	2.29	7/25	PW6B95 (1.78)	13 compounds	6 atoms and 7 molecules	38.16	MG3S	80
	3.4	3/5	c-SVWNV (2.6)	58 compounds	58 atoms and molecules from the G3 test set	32.55	6-311+G**	106
	3.5	3/37	B98 (3.2)	25 compounds	derived from the Gaussian G2/97 test set	n/a	Aug-cc-pVTZ	108
E. heats of formation	27.1	30/42	mPWPW91 (9.5)	372 compounds	372 containing 5 or fewer heavy atoms	45.9	MIDI!	111
	17.8	2/6	BLYP (15.0)	223 compounds	223 molecules from the G3 test set	50.9	6-311+G**	106
	7.0	8/37	B3PW91 (3.95)	156 compounds	derived from the Gaussian G2/97 test set	n/a	Aug-cc-pVTZ	108
	3.31	3/23	B98 (2.90)	148 compounds	148 molecules from the G2/97 test set	49.0	6-311+G(3d2f,2p)	112
E. isomerizations	6.24	17/25	M05 (1.84)	3 pairs of compounds	3 pairs of cumulenes and poly-ynes Isomers	8.17	6-311+G(2df,2p)	113

TABLE 3 (Continued)

| | B3LYP | | best results | | | av. value in | | |
	MUE	ranking	functional (MUE)	dataset size	dataset characteristics	the dataset[a]	basis set	ref
Nonbonded Interactions I[b] (kcal/mol)								
A. H bonding	0.45	4/15	B97-1 (0.26)	4 binding energies	4 H-bonding dimers	9.38	MG3S	70
	1.94	6/6	PWB6K (0.46)	5 binding energies	5 π H-bonding systems	4.49	MG3S	114
	0.77	21/44	B3P86 (0.46)	6 binding energies	6 H-bonding dimers	8.37	DIDZ/aug-cc-pVTZ/MG3S	71
	0.76	18/25	PBE1PBE (0.34)	6 binding energies	6 H-bonding dimers	8.37	MG3S	80
	0.65	9/37	MPWLYP (0.31)	10 binding n energies	10 H-bonding systems	7.15	Aug-cc-pVTZ	108
B. charge transfer	0.80	9/44	MPWB1K (0.50)	7 binding energies	7 charge-transfer complexes	4.63	DIDZ/aug-cc-pVTZ/MG3S	71
	0.63	9/25	PWB6K (0.21)	7 binding energies	7 charge-transfer complexes	4.63	MG3S	80
C. dipole interactions	0.78	29/44	PBE1KCIS (0.36)	6 binding energies	6 dipole-interaction complexes	3.05	DIDZ/aug-cc-pVTZ/MG3S	71
	0.86	20/25	PWB6K (0.28)	6 binding energies	6 dipole-interaction complexes	3.05	MG3S	80
Nonbonded Interactions II[c] (kcal/mol)								
A. weak interactions	0.23	15/15	B97-1 (0.02)	4 binding energies	4 rare-gas dimers	0.08	MG3S	70
	0.60	32/44	B97-1 (0.19)	9 binding energies	9 weak-interaction complexes	0.47	DIDZ/aug-cc-pVTZ/MG3S	71
	0.35	21/25	B97-1 (0.10)	7 binding energies	7 weak-interaction complexes	0.22	MG3S	80
			M05-2X (0.12)	10 binding energies	10 rare-gas dimers	0.16	Aug-cc-pVTZ	115
B. π-π interactions	8.52	6/6	PWB6K (1.86)	11 binding energies	6 nucleic acid bases complexes + 5 amino acid pairs	7.53	DIDZ	72
	3.06	24/25	PWB6K (0.90)	5 binding energies	5 π-π stacking complexes	2.02	MG3S	80

[a] Average value of the property in the dataset used for evaluation. [b] Nonbonded interactions in which electrostatic or orbital-orbital interactions are dominant and the dispersion contribution is small. [c] Nonbonded interactions in which the dispersion contribution is dominant.

mean unsigned error (MUE) was obtained with BPW91 (0.007 Å, for the aug-cc-pV5Z basis set), closely followed by BP86 and B3LYP (MUE = 0.008 Å).

Zhao and Truhlar[70] have evaluated the performance of 12 density functionals in the determination of saddle point geometries, considering a dataset of five hydrogen-transfer reactions (10 bond lengths in total), for which very-high level calculations of saddle point geometries were available. In this study, the best results in the determination of bond lengths (MG3S basis set) were obtained with MPW1K (MUE = 0.01 Å). XB1K, BB1K, MPWB1K also rendered very good results (MUE = 0.02 Å), whereas B3LYP (MUE = 0.06 Å) gave the worst MUE of the set of 12 density functionals tested.

Riley et al.[106] have compared six density functionals (Slater, SVWNV, BLYP, B3LYP, and c-SVWNV) in the determination of bond lengths, considering a dataset of 32 small neutral molecules (44 experimentally determined bond lengths). In this study (basis set 6-311+G**), B3LYP gave the best results, with a MUE of 0.008 Å, and was followed by c-SVWNV and BLYP (MUE of 0.013 and 0.015 Å).

The performance of 42 functionals in the calculation of 13 metal−ligand bond lengths was recently analyzed by Schultz et al.[67] The molecules used for bond length comparison were AgH, BeO, CoH, CoO$^+$, FeO, FeS, LiCl, LiO, MgO, RhC, VO, and VS. In the determination of metal−ligand bond lengths with both double-ζ quality (DZQ) and a triple-ζ quality (TZQ) basis sets, the best results were obtained with MPW3LYP, X3LYP, TPSSh, and TPSS1KCIS (MUE = 0.013 Å), closely followed by B3LYP (MUE = 0.014 Å), which was ranked fifth in the test.

Schultz et al.[107] have tested the ability of 42 density functionals in geometry determination for 8 metal dimers (Ag$_2$, Cr$_2$, Cu$_2$, CuAg, Mo$_2$, Ni$_2$, V$_2$, and Zr$_2$) with DZQ and a TZQ basis sets. The lowest average MUE in bond lengths was obtained with SPWL and SVWN3 (MUE = 0.05 Å). In the GGA methods, BP86, G96LYP, mPWLYP, and X3LYP were the most successful (MUE = 0.07 Å), whereas BB95 came first among the M-GGAs (MUE = 0.07 Å), and B97-2 among the H-GGAs (MUE = 0.15 Å). B1B95, TPSSh, and TPSS1KCIS gave the best results among the HM-GGAs (MUE = 0.14 Å). B3LYP resulted in an MUE of 0.16 Å (27th position out of 42 density functionals in the test). These results highlight a marked difference between the MUEs typically encountered for small organic molecules (as described in Wang and Wilson[105]), and the ones calculated for metal compounds Schultz et al.[107] Even though these two sets of results are not directly comparable, as the basis sets employed largely differ (aug-cc-pV5Z in Wang and Wilson, and DZQ and TZQ in Schultz et al.), the error involved in geometry determination of metal systems is normally higher than the one associated with calculations of small organic molecules.

A recent study by Riley et al.[108] has compared the performance of 37 density functionals in the determination of 71 bond lengths of 44 small organic molecules whose structures are well characterized experimentally. In this study, the best performance with the aug-cc-pVQZ was obtained with VSXC (MUE = 0.006 Å), with B3LYP closely following (MUE = 0.007 Å) and yielding the second best result.

Angles. Wang and Wilson[105] have evaluated the performance of six well-established density functionals (B3LYP, B3PW91, B3P86, BLYP, BPW91, and BP86) in the determination of molecular geometries. In particular, a total of 10 experimentally derived bond angles of first-row closed-shell molecules of relevance in atmospheric chemistry were considered. The best

Review Article

J. Phys. Chem. A, Vol. 111, No. 42, 2007 **10447**

results in this test (aug-cc-pV5Z basis set) were obtained with B3LYP (MUE = 0.75°), followed by BLYP (MUE = 0.77°) and B3P86 (MUE = 0.81°).

Riley et al.[106] compared six density functionals (Slater, SVWNV, BLYP, B3LYP, and c-SVWNV) in the calculation of 16 bond angles of small neutral molecules. C-SVWNV and SVWNV gave the best results of the test (MUE = 1.82° with the 6-311+G** basis set), with B3LYP coming in the fifth position with a MUE of 1.94°.

A dataset of 34 bond angles of 27 small organic molecules was used by Riley et al.[108] to assess the ability of 37 density functionals to correctly reproduce geometries. In this test, the best results in the calculation of bond angles with the aug-cc-pVQZ basis set were obtained with PBE1PBE (1.11°) and B3P86 (MUE = 1.12°). B3LYP was ranked 11th in the test, with a MUE of 1.20°.

Nonbonded Interactions. The performance of 15 density functionals in the determination of the correct geometries for hydrogen bonds, was evaluated by Zhao and Truhlar[70] by considering a dataset comprising four hydrogen-bonding dimers, with values taken from high-level calculations or experimental results. These dimers were $(HF)_2$, $(H_2O)_2$, $(HCOOH)_2$, and $(HCONH_2)_2$. In this test (MG3S basis set), MPW3LYP gave the lowest MUE for hydrogen-bonding distances (0.01 Å), followed by MPW1B95, B97-1, MPWB1K, XB1K, X3LYP, and B3LYP (MUE = 0.02 Å).

A dataset of four rare-gas dimers (HeNe, NeNe, HeAr, and NeAr) was also used by Zhao and Truhlar[70] to analyze the ability of 15 density functionals to reproduce weak interaction distances. In this study (MG3S basis set), B3LYP gave the worst result of the test, systematically overestimating to a large extent the weak interaction distance (mean signed error, MSE = MUE = 1.02 Å). The best performances were obtained with B97-1 (MUE = 0.08 Å), and with B98, MPW1B95, and MPWB1K (MUE = 0.09 Å).

Kinetics. *Barrier Heights.* A total of 22 density functionals were compared considering a representative dataset of six barrier heights by Zhao et al.[109] This dataset comprises the forward and reverse barrier heights for three hydrogen-transfer reactions. In this study, MPW1K was shown to give the best results with the MG3S basis set (MUE = 1.4 kcal/mol), followed by B1B95 (MUE = 3.1 kcal/mol), and B97-2 (MUE = 3.2 kcal/mol). B3LYP was ranked 11th in the test, with a MUE of 4.7 kcal/mol.

The ability of 15 density functionals to calculate barrier heights with the MG3S basis set was evaluated by Zhao and Truhlar[70] for a dataset of 42 reactions, comprising mainly open-shell hydrogen-transfer processes. The best results were obtained with BB1K (MUE = 1.16 kcal/mol), XB1K (MUE = 1.23 kcal/mol), and MPWB1K (MUE = 1.29 kcal/mol). All the density functionals tested underestimated the barrier heights, particularly MPW3LYP (MSE = −4.76 kcal/mol) and B3LYP (MSE = −4.40 kcal/mol). B3LYP gave a MUE of 4.31 kcal/mol and was ranked 14th in the test.

Zhao and Truhlar[80] have also analyzed the performance of 25 density functionals in the calculation of 38 transition-state barrier heights for non-hydrogen-transfer reactions. These included 12 heavy-atom-transfer reactions, 16 nucleophilic substitution reactions, and 10 non-nucleophilic unimolecular and association reactions. The average barrier height for this database was 22.98 kcal/mol. The application of these functionals in the determination of 38 transition-state barrier heights for hydrogen-transfer reactions was also evaluated (average barrier height 13.26 kcal/mol). Both studies were performed with the MG3S

basis set. For heavy-atom-transfer reactions, the best results were obtained with BB1K (MUE = 1.58 kcal/mol), PWB6K (MUE = 1.61 kcal/mol), MPWB1K (MUE = 1.69 kcal/mol), and MPW1K (MUE = 1.89 kcal/mol), whereas in nucleophilic substitution reactions B1B95 (MUE = 1.08 kcal/mol), PWB6K (MUE = 1.10 kcal/mol), and MPWKCIS1K (MUE = 1.17 kcal/mol) gave the lowest errors. In the non-nucleophilic unimolecular and association reactions, the best performance in the calculation of barrier heights was achieved with B1B95 (MUE = 1.21 kcal/mol), MPW1B95 (MUE = 1.31 kcal/mol), and PW6B95 MUE = 1.43 kcal/mol). For the set of 38 hydrogen-transfer reactions, the best results were obtained with BB1K (MUE = 1.16 kcal/mol), PWB6K (MUE = 1.28 kcal/mol), MPWB1K (MUE = 1.29 kcal/mol), and MPW1K (MUE = 1.32 kcal/mol), which also gave the best overall results in the set of 76 barrier heights considered (overall MUE of 1.50, 1.59, 1.60, and 1.82 kcal/mol). B3LYP was shown to systematically underestimate the barrier heights, particularly in heavy-atom-transfer reactions (MSE = −8.49 kcal/mol). From the 25 density functionals tested, B3LYP was ranked 16th in the calculation of barrier heights for heavy-atom-transfer reactions (MUE = 8.49 kcal/mol), 16th for nucleophilic substitutions (MUE = 3.25 kcal/mol), 13th in the non-nucleophilic unimolecular and association reactions (MUE = 2.02 kcal/mol), and 15th in hydrogen-transfer reactions (MUE = 4.23 kcal/mol). In the total of 76 barrier heights considered B3LYP was ranked 15th, with an average MUE of 3.08 kcal/mol, against an average MUE of 1.50 kcal/mol by BB1K, the best functional in the test.

Schultz et al.[107] have evaluated the performance of 42 density functionals in the calculation of six barrier heights considering a representative dataset of hydrogen-transfer reactions and using the MG3S basis set. In this test, BB1K gave the best results (MUE = 1.14 kcal/mol), closely followed by MPWKCIS1K (MUE = 1.20 kcal/mol). B3LYP resulted in an MUE of 4.73 kcal/mol (17th position in the test).

Zhao et al.[68] have evaluated the performance of 29 density functionals in the determination of the barrier heights for 76 reactions (38 hydrogen-transfer reactions plus 38 non-hydrogen-transfer reactions), using the MG3S basis set. The best results were obtained with BB1K (MUE = 1.37 kca/mol) and MPW1K (MUE = 1.73 kcal/mol). B3LYP rendered a MUE of 4.50 kcal/mol (17th out of 29 functionals).

A recent study by Riley et al.[108] has compared 37 density functionals in the calculation of barrier heights for 23 reactions of small systems with radical transition states. In this study, the best result with the aug-cc-pVTZ basis set was obtained with BB1K (MUE = 1.05 kcal/mol), with B3LYP coming in seventh position out of the 37 functional tested with a MUE of 4.30 kcal/mol. This study has also compared the performance of these 37 density functionals in the determination of barrier heights for six reactions of larger systems with a singlet transition state, using also the aug-cc-pVTZ basis set. In this second test, the lowest MUE was obtained with B1LYP (2.58 kcal/mol), with B3LYP occupying the second position in the test (MUE = 3.10 kcal/mol).

Thermochemistry. *Atomization Energies.* A total of six density functionals was evaluated by Wang and Wilson[105] in the calculation of the atomization energies for 17 first-row closed-shell molecules of interest in atmospheric chemistry. The functionals tested were B3LYP, B3PW91, B3P86, BLYP, BPW91, and BP86. B3LYP gave the lowest MUE (2.19 kcal/mol) with the aug-cc-pV5Z basis set, followed by B3PW91 (MUE = 2.24 kcal/mol), and BLYP (MUE = 7.22 kcal/mol), with BP86 giving the worst results (MUE = 16.19 kcal/mol).

The performance of 22 density functionals in the determination of atomization energies was evaluated by Zhao et al.[109] considering a representative database of six organic molecules (SiH_4, SiO, S_2, C_3H_4, $C_2H_2O_2$, and C_4H_8). In this study, the best performance with the MG3S basis set was obtained with VSXC and O3LYP (MUE = 0.5 kcal/mol), closely followed by B1B95, B3PW91 (MUE = 0.6 kcal/mol), B3LYP, and B97-2 (MUE = 0.7 kcal/mol).

A database comprising the atomization energies for a total of 109 molecules, including both organic and inorganic compounds (but no transition metals) was used by Zhao and Truhlar[70] to compare the performance of 15 density functionals using the MG3S basis set. The best results were obtained with X1B95 (MUE = 0.52 kcal/mol), closely followed by B1B95 (MUE = 0.56 kcal/mol). B3LYP was ranked ninth in the test with an MUE of 0.90 kcal/mol.

The same dataset of atomization energies for 109 molecules composed of main group elements was used by Zhao and Truhlar in another study[80] to analyze the performance of 25 density functionals with the MG3S basis set. In this test PW6B95 gave the lowest MUE (0.40 kcal/mol), followed by B1B95 (MUE = 0.55 kcal/mol), MPW1B95 (MUE = 0.62 kcal/mol), and B98 (MUE = 0.64 kcal/mol). B3LYP was ranked 12th in the test (MUE = 0.91 kcal/mol).

Schultz et al.[107] have analyzed the performance of 42 density functionals in the calculation of the atomization energies of nine metal dimers (Ag_2, Cr_2, Cu_2, $CuAg$, Mo_2, Ni_2, V_2, Zr_2, and ZrV) with a DZQ and a TZQ basis sets. In this study the best results were obtained with the B97-2 and BLYP functionals (MUE = 5.3 kcal/mol), with B3LYP coming in the 29th position with an impressive MUE of 16.7 kcal/mol. The performance of these 42 density functionals was also compared with the results from the calculation of the atomization energies of six organic molecules with the MG3S basis set. These molecules were SiH_4, SiO, S_2, C_3H_4, $C_2H_2O_2$, and C_4H_8. The best result was obtained with MPW3LYP (MUE = 0.43 kcal/mol), followed by B98 (MUE = 0.50 kcal/mol), and B1B95 (MUE = 0.60), with B3LYP coming in the fourth position (MUE = 0.61 kcal/mol).

The same dataset of atomization energies for nine metal dimers was applied in another study, following a slightly different protocol, by Schultz et al.[67] to compare the performance of 42 density functionals. In this second study, also with a DZQ and a TZQ basis sets, BLYP gave the best results (MUE = 5.8 kcal/mol), followed by XLYP (6.8 kcal/mol) and mPWLYP (MUE = 7.2 kcal/mol). B3LYP was ranked 27th out of the 42 functionals tested with a MUE of 26.3 kcal/mol.

Binding Energies. The performance of 42 functionals in the calculation of 21 bond dissociation energy potentials for transition metal compounds was analyzed by Schultz et al.[67] The molecules for which the metal−ligand dissociation energy was evaluated were AgH, CoH, CoO^+, $CoOH^+$, $CrCH_3^+$, $CuOH_2^+$, FeH, $Fe(CO)_5$, FeO, FeS, LiCl, LiO, MgO, $MnCH_3^+$, $NiCH_2^+$, $Ni(CO)_4$, RhC, VCO^+, VO, and VS. The most accurate bond dissociation energies, considering the DZQ and TZQ basis sets, were obtained with TPSS1KCIS (MUE = 5.4 kcal/mol), O3LYP (MUE = 5.5 kcal/mol), and MPW1KCIS (MUE = 5.6 kcal/mol), with B3LYP performing relatively well (MUE = 6.5 kcal/mol) (10th out of 42 density functionals).

Zhao and Truhlar[110] have evaluated the performance of seven density functionals (B3LYP, B97-2, BLYP, M05, MPWLYP1M, TPSS, and TPSSh) with the QZVP basis set, in the determination of 12 binding energies of dimers involving transition metal atoms (Sc_2, V_2, Ni_2, CrH, MnH, CoH, TiO, MnO, CuO, ScF, CrF, CuF) and six reaction energies. The results showed that

the hybrid functionals B97-2, M05, and B3LYP gave better results in the calculation of the binding energies of the monohydrides, monoxides, and monofluoride dimers. However, in the calculation of the binding energy for the Sc_2, V_2, and Ni_2 dimers TPSS showed the best performance, followed by MPWLYP1M. Globally, for all 18 data evaluated, M05 gave the best results (MUE = 7.8 kcal/mol), closely followed by B97-2 (MUE = 8.3 kcal/mol), whereas B3LYP came last (MUE = 12 kcal/mol).

Ionization Potentials. The ionization potentials of a dataset comprising six atoms (C, S, Cl, O, P, Si) and seven molecules (SH, Cl_2, OH, O_2, PH, PH_2, S_2), were used to analyze the performance of 15 density functionals by Zhao and Truhlar[70] using the MG3S basis set. The lowest MUE was obtained with MPWB1K (2.05 kcal/mol), closely followed by BB1K (MUE = 2.09 kcal/mol) and MPW1B95 (MUE = 2.14 kcal/mol). B3LYP, with a MUE of 4.72 kcal/mol, was ranked 14th out of the 15 functionals tested.

Zhao and Truhlar[80] have used this same dataset to compare 25 density functionals. In this study, the best performance in the calculation of ionization potentials with the MG3S basis set was obtained again with MPWB1K (MUE = 2.05 kcal/mol), BB1K (MUE = 2.09 kcal/mol), and MPW1B95 (MUE = 2.14 kcal/mol), with B3LYP coming in the 18th position out of 25 density functionals (MUE = 4.72 kcal/mol).

The performance of five density functionals (Slater, SVWNV, BLYP, B3LYP, and c-SVWNV) in the determination of ionization potentials was compared for a total of 88 atoms and molecules from the Gaussian G3 test set by Riley et al.[106] In this test, the best results with the 6-311+G** basis set were obtained with B3LYP (MUE = 3.8 kcal/mol), followed by c-SVWNV and SVWNV with a MUE of 4.7 and 5.2 kcal/mol, respectively.

Schultz et al.[67] have evaluated the performance of 57 density functionals in the calculation of ionization potentials, considering a dataset of seven atoms and using the DZQ and TZQ basis sets. The atoms used in the calculation of atomic ionization potentials were C, Co, Cr, Cu, Ni, O, and V. For the calculation of ionization potentials OLYP (AMUE = 3.1 kcal/mol), B1B95 (MUE = 3.6 kcal/mol), O3LYP (MUE = 3.6 kcal/mol), and MPW1B95 (MUE = 3.6 kcal/mol) gave the best results, whereas the popular B3LYP functional had a modest performance (MUE = 7.2 kcal/mol) and was ranked 27th.

A dataset composed of 37 atoms and molecules was used by Riley et al.[108] to evaluate the ability of 37 density functionals to calculate ionization potentials using the aug-cc-pVTZ basis set. The values for 36 of these 37 compounds were taken from the Gaussian G2/97 test set. To increase the contribution of phosphorus containing systems, a non-G2 compound (PO_2) was added to the test set. The best results were obtained with B1B95 (MUE = 4.25 kcal/mol), whereas B3LYP was ranked 13th of the test (MUE = 5.10 kcal/mol).

Electron Affinities. The accuracy of 15 density functionals in the calculation of electron affinities was analyzed for six atoms (C, S, Cl, O, P, Si) and seven molecules (SH, Cl_2, OH, O_2, PH, PH_2, S_2) by Zhao and Truhlar.[70] In this study, the best results with the MG3S basis set were obtained with B98 (MUE = 1.84 kcal/mol), B97-1 (MUE = 2.02 kcal/mol), and MPW3LYP (MUE = 2.14 kcal/mol), with B3LYP yielding the fourth best result (MUE = 2.29 kcal/mol).

Another study by Zhao and Truhlar[80] has evaluated the performance of 25 density functionals in the determination of electron affinities with the MG3S basis set for the same dataset of six atoms and seven molecules. PW6B95 (MUE = 1.78 kcal/

mol), B98 (MUE = 1.84 kcal/mol), B97-1 (MUE = 2.02 kcal/mol), and MPW3LYP (MUE = 2.02 kcal/mol) gave the best performance for the calculation of electron affinities. B3LYP (MUE = 2.29 kcal/mol) was ranked seventh in this test.

The performance of five density functionals (Slater, SVWNV, BLYP, B3LYP, and c-SVWNV) in the determination of electron affinities was compared for a total of 58 atoms and molecules from the Gaussian G3 test set by Riley et al.[106] In this study, the best performance with the 6-311+G** basis set was obtained with c-SVWNV (MUE = 2.6 kcal/mol), followed by BLYP (MUE = 3.1 kcal/mol) and B3LYP (MUE of 3.6 kcal/mol).

A more recent study by Riley et al.[108] has compared the performance of 37 density functionals in the determination of the electron affinity for 25 atoms and molecules with the aug-cc-pVTZ basis set. The values for 24 of these 25 compounds were taken from the Gaussian G2/97 test set. A non-G2 compound (PO_2) was added to the test set to increase the contribution of phosphorus containing systems. The lowest MUE in this study was obtained with B98 (3.15 kcal/mol). B3LYP was ranked third in the test, with a MUE of 3.5 kcal/mol.

Heats of Formation. The performance of 32 density functionals in the determination of the heat of formation for 372 compounds containing five or fewer heavy atoms and consisting of atoms H, C−F, and P−Cl taken from the NIST thermochemical database was analyzed by Brothers and Merz.[111] They showed that mPWPW91 and B3P86 give the lowest MUE in the set of 32 density functionals tested (MUE of 9.5 and 9.6 kcal/mol with the MIDI! basis set), whereas B3LYP was ranked 30th with a rather poor MUE of 27.1 kcal/mol.

Six density functionals have been evaluated in the determination of the heat of formation for a total of 223 molecules from the Gaussian G3 test set by Riley et al.[106] In this study, the lowest MUE with 6-311+G** was obtained with BLYP (15.0 kcal/mol), followed by B3LYP and c-SVWNV (MUE of 17.8 and 19.6, respectively).

A more recent study by Riley et al.[108] has compared the performance of 37 density functionals in the determination of the heat of formation for 156 atoms and molecules using the aug-cc-pVTZ basis set, with reference values taken almost exclusively from the G2/97 test set. The exceptions were PH, PO_2, and CH_3PH_2. B3LYP (MUE = 7.0 kcal/mol) was ranked eighth out of the 37 density functionals considered in this study, with B3PW91 yielding the best result (MUE = 3.95 kcal/mol).

Curtiss and Redfern[112] have evaluated the performance of 23 density functionals in the calculation of the enthalpies of formation for 148 molecules from the G2/97 test set using the 6-311+G(3d2f,2p) basis set. In this study, the best performance was obtained with B98 (MUE = 2.90 kcal/mol), followed by X3LYP and B3LYP (MUE of 3.26 and 3.31 kcal/mol).

Other Reaction Energies. A recent study by Zhao and Truhlar[113] has systematically compared the performance of 25 density functionals in the calculation of the energy differences between three pairs cumulenes and poly-yne isomers using the 6-311+G(2df,2p). In the calculation of the energy differences between cumulenes and poly-yne isomers, the most accurate results were obtained with the very recent functionals M05 (MUE = 1.84 kcal/mol), OHandHB95 (MUE = 2.60 kcal/mol), and M05-2X (MUE = 2.99 kcal/mol), with B3LYP ranking 17th out of 25 (MUE = 6.24 kcal/mol).

Nonbonded Interactions. The performance of the currently available density functionals will be analyzed by considering two different groups of nonbonded interactions. The first group contains the nonbonded interactions where the dispersion contribution is not very significant, and that are characterized by a dominant contribution by the electrostatic and orbital−orbital interactions. This group includes hydrogen bonding, charge transfer, and dipole interactions. The second group of nonbonded interactions comprises those in which dispersion is the major source of attraction and includes weak interactions and $\pi-\pi$ interactions.

Hydrogen Bonding. A total of 15 density functionals were analyzed in the determination of the binding energies of four hydrogen-bonding dimers by Zhao and Truhlar.[70] These dimers were $(HF)_2$, $(H_2O)_2$, $(HCOOH)_2$, and $(HCONH_2)_2$. In this study, performed with the MG3S basis set, B97-1 (MUE = 0.26 kcal/mol), X3LYP (MUE = 0.34 kcal/mol), and B98 (MUE = 0.38 kcal/mol) gave the lowest MUE, closely followed by B3LYP (MUE = 0.45 kcal/mol), which was ranked fourth out of the 15 density functionals tested.

The recently developed density functionals MPW1B95, MPWB1K, PW6B95, and PWB6K were tested against B3LYP and PW91 using the MG3S basis set for six π hydrogen-bonded systems by Zhao et al.[114] These were $H_2O-C_6H_6$, $NH_3-C_6H_6$, $HCl-C_6H_6$, H_2O-indole, and H_2O-methylindole. The results showed that MPW1B95, MPWB1K, PW6B95, and PWB6K give accurate energetics for π hydrogen-bonding interactions, whereas B3LYP fails (MUE = 1.94 kcal/mol for an average database value of 4.49 kcal/mol) and PW91 (MUE = 0.91 kcal/mol) is less accurate. PWB6K was the most accurate density functional of the test with a MUE of 0.46 kcal/mol in the calculation of binding energies.

The performance of 44 density functionals has been evaluated in the determination of the binding energies of six hydrogen-bonding dimers by Zhao and Truhlar[71] with the DIDZ, aug-cc-pVTZ, and MG3S basis sets. The dimers considered in the database were $(NH_3)_2$, $(HF)_2$, $(H_2O)_2$, NH_3-H_2O, $(HCONH_2)_2$, and $(HCOOH)_2$. PBE (MUE = 0.50 kcal/mol) gave the most accurate results, among the LDA and GGA functionals, whereas VSXC (MUE = 0.61 kcal/mol) and TPSS (MUE = 0.66 kcal/mol) came first in the M-GGAs. In the H-GGA, the best performance was achieved with the B3P86 (MUE = 0.46 kcal/mol) and PBE1PBE (MUE = 0.47 kcal/mol) functionals, whereas B3LYP (MUE = 0.77 kcal/mol) was ranked 10th out of 13 H-GGA functionals (21st overall). Among the HM-GGA functionals the most accurate results were obtained with PBE1KCIS (MUE = 0.60 kcal/mol) and MPWB1K (MUE = 0.61 kcal/mol). The two DFT methods tested that included the OptX exchange functional (OLYP and O3LYP) gave particularly bad results for hydrogen-bonding dimers (MUE of 3.60 and 2.76 kcal/mol, respectively). Altogether, the best results in the determination of the binding energies hydrogen-bonding dimers were obtained with B3P86 (MUE = 0.46 kcal/mol) and PBE1PBE (MUE = 0.47 kcal/mol).

Another study by Zhao and Truhlar[80] has compared the performance of 25 density functionals against these same six hydrogen-bonding dimers using the MG3S basis set. The best results were obtained with PBE1PBE (MUE = 0.34 kcal/mol), PBE (MUE = 0.39 kcal/mol), and PWB6K (MUE = 0.39 kcal/mol). B3LYP came on the 18th position among the 25 functionals tested (MUE = 0.76 kcal/mol).

The performance of 37 density functionals in the determination of the binding energies for ten hydrogen-bonding systems was recently evaluated by Riley et al.[108] The test set here included ten hydrogen-bonding systems whose interaction energies had been well characterized by high-level theoretical techniques. The results using the aug-cc-pVTZ pointed out MPWLYP as the most accurate method (MUE = 0.31 kcal/mol), closely followed by PBE1KCIS (MUE = 0.36 kcal/mol).

B3LYP, with an MUE of 0.65 kcal/mol, was ranked ninth out of 37 in the test.

Charge Transfer. The binding energies of seven charge-transfer complexes have been used to test the application of 44 density functionals by Zhao and Truhlar[71] with the DIDZ, aug-cc-pVTZ, and MG3S basis sets. The database consisted of seven charge-transfer complexes $C_2H_4-F_2$, NH_3-F_2, C_2H_2-CIF, $HCN-CIF$, NH_3-Cl_2, H_2O-CIF, and NH_3-CIF. From the 3 LDA and 12 GGA methods tested, the best result was obtained with G96LYP (MUE = 1.33 kcal/mol), whereas BB95 (MUE = 1.56 kcal/mol) was ranked first in the M-GGAs. Within the 15 H-GGA functionals evaluated, the highest accuracy was obtained with BHandLYP (MUE = 0.63 kcal/mol) and MPW1K (MUE = 0.68 kcal/mol), with B3LYP ranking fifth (MUE = 0.80 kcal/mol, ninth overall). The best overall performance in the test for calculating the binding energies of charge-transfer complexes was obtained with the HM-GGAs MPWB1K (MUE = 0.50 kcal/mol) and MPW1B95 (MUE = 0.56 kcal/mol) functionals. All the LDA, GGA, and M-GGA functionals tested have been shown to systematically overestimate the binding energies of the charge-transfer complexes considered.

The performance of 25 density functionals was also tested on another study by Zhao and Truhlar[80] against this database of binding energies for seven charge-transfer complexes using the MG3S basis set. In this test, PWB6K and MPWB1K gave the best results (MUE of 0.21 and 0.34 kcal/mol), whereas B3LYP was ranked ninth (MUE = 0.63 kcal/mol).

Dipole Interactions. Zhao and Truhlar[71] have assessed the performance of 44 density functionals in the treatment of dipole interactions by considering the binding energy of six dipole interaction complexes with the DIDZ, aug-cc-pVTZ, and MG3S basis sets. These dipole interaction complexes were $(H_2S)_2$, $(HCl)_2$, $HCl-H_2S$, $CH_3Cl-HCl$, $CH_3SH-HCN$, and $CH_3SH-HCl$. mPWLYP yielded the lowest MUE (0.41 kcal/mol) among the GGA functionals, with PBEKCIS (0.41 kcal/mol) giving the best result within the M-GGAs. B97-1 and MPW3LYP were the best H-GGAs, with MUE of 0.33 and 0.34 kcal/mol, respectively, and were actually the best functionals of the study for the treatment of dipole interactions. B3LYP (MUE = 0.78 kcal/mol) was ranked ninth out of the 15 H-GGAs (29th overall). Among the HM-GGAs, the best result was obtained with PBE1KCIS (MUE = 0.36 kcal/mol).

Another study by Zhao and Truhlar[80] has analyzed the performance of 25 density functionals in the calculation of these binding energies for dipole interaction complexes using the MG3S basis set. PWB6K gave the best result (MUE = 0.28 kcal/mol), closely followed by B97-1 (MUE = 0.29 kcal/mol). B3LYP was ranked 20th out of 25 in the test (MUE = 0.86 kcal/mol).

Weak Interactions. The performance of 15 density functionals in the treatment of weak interactions was compared by Zhao and Truhlar[70] by considering a dataset of four binding energies for rare-gas dimers (HeNe, NeNe, HeAr, and NeAr). The average energy value of this dataset is 0.08 kcal/mol. In this study, B97-1, B98, and MPWB1K (MUE = 0.02 kcal/mol) gave the best results with the MG3S basis set. B3LYP (MUE = 0.23 kcal/mol) gave the worst result in the test, among the 15 density functionals tested.

The binding energy of nine weak interaction complexes was used to compare the performance of a total of 44 density functionals by Zhao and Truhlar[71] using the DIDZ, aug-cc-pVTZ, and MG3S basis sets. The nine weak interaction complexes considered were HeNe, NeNe, HeAr, NeAr, CH_4-Ne, C_6-H_6-Ne, $(CH_4)_2$, $(C_2H_2)_2$, and $(C_2H_4)_2$. In this study,

PBE came first in the test, among the LDA and GGA functionals, with a MUE of 0.28 kcal/mol. The best M-GGA for the treatment of weak interactions was PBEKCIS (MUE = 0.27 kcal/mol), whereas B97-1 came first among the H-GGAs (MUE = 0.19 kcal/mol), and was the best functional in the test. B3LYP with a MUE of 0.60 kcal/mol occupied the 10th position among the 15 H-GGAs considered (32nd overall). Finally, MPWB1K was ranked first among the 9 HM-GGA methods tested (MUE = 0.22 kcal/mol). The mean value of the binding energy for the nine complexes tested was 0.47 kcal/mol. So even the use of the best method in the test (B97-1) resulted in an error of 40%, clearly illustrating the limitations of current density functionals in dealing with van der Waals interactions.

Another study by Zhao and Truhlar[80] focusing on the binding energies of seven weak interaction complexes compared a total of 25 density functionals using the MG3S basis set. The dataset in this study included HeNe, NeNe, HeAr, NeAr, CH_4-Ne, C_6-H_6-Ne, and $(CH_4)_2$. In this test, the best performance was obtained with PW6B95 and B97-1 (MUE = 0.10 kcal/mol), whereas B3LYP (MUE = 0.35 kcal/mol) was ranked 21st in the test.

A total of 18 density functionals were tested in the analysis of van der Waals interactions in ten rare-gas dimers, three alkaline-earth-metal dimers, the zinc dimer, and three zinc-rare gas dimers by Zhao and Truhlar[115] using the aug-cc-pVTZ basis set. B97-1, PBEPW91, and B98 gave the best results for the geometry optimization of the ten rare-gas dimers (MUE = 0.14 Å), whereas M05-2X, B97-1, B98, and PBE yielded the most accurate binding energies (MUE of 0.053, 0.069, 0.080, and 0.082 kcal/mol, respectively). For the alkaline-earth-metal dimers and zinc dimers, M05-2X and PWB6K gave the best results for geometry optimization (MUE = 0.21 Å) and calculation of the binding energies (MUE of 0.12 and 0.20 kcal/mol, respectively). The best overall performance of the test was obtained with the M05-2X and MPWB1K functionals.

π−π Interactions. Six nucleic acid base complexes and five amino acid pairs have been used by Zhao and Truhlar[72] to compare the performance of six density functionals in the treatment of π−π interactions in biological systems using the DIDZ basis set. The functionals tested were B3LYP, B97-1, MPW1B95, MPWB1K, PW6B95, and PWB6K. PWB6K gave the best estimate (MUE = 1.86 kcal/mol), followed by MPWB1K (MUE = 2.68 kcal/mol) and PW6B95 (MUE = 2.84 kcal/mol). B3LYP and B97-1 clearly fail in describing the π−π interactions in these complexes (MUEs of 8.52 and 5.65 kcal/mol, respectively, for an average database value of 7.53 kcal/mol).

Another study by Zhao and Truhlar[80] has evaluated the performance of 25 density functionals in the calculation of the binding energy of five π−π stacking complexes using the MG3S basis set. The complexes considered were $(C_2H_2)_2$, $(C_2H_4)_2$, sandwich $(C_6H_6)_2$, T-shaped $(C_6H_6)_2$, and parallel-displaced $(C_6H_6)_2$. The best results were obtained with PWB6K (MUE = 0.90 kcal/mol), followed by PW6B95 (MUE = 1.32 kcal/mol), and MPWB1K (MUE = 1.45 kcal/mol). B3LYP (MUE = 3.06 kcal/mol for an average value of the binding energy in the dataset of 2.02 kcal/mol) was ranked 24th out of the 25 density functionals (the worst functional being BLYP).

General Comments. Table 3 presents a summary of the benchmarking studies on density functionals published during the past 4 years, illustrating the relative performance of the popular B3LYP functional among the several density functionals tested in the 57 comparisons discussed above. It also indicates the best functional in each study, the correspondent MUE, and

Review Article

J. Phys. Chem. A, Vol. 111, No. 42, 2007 **10451**

the mean value (magnitude) of the databases used for each property. Rather than providing an indication of the best functional for each property, or an accurate ranking situating B3LYP in the plethora of existing density functionals, Table 3 tries to give an indication of the level of accuracy that might be expected with B3LYP for each individual property, and the best performance that can be presently obtained with a density functional. The multitude of different parameters involved in each study renders impossible a more systematic comparison of the results obtained in the set of studies analyzed. In this context, the specific ranking of B3LYP within each study should be regarded simply as a first and rough indicator of its relative accuracy for each property, among the available alternatives, with the position within each ranking varying according to aspects like the number and sophistification of the alternatives tested, the dataset considered, the basis sets used, and the protocol followed. Also, the particular ranking of a given functional may change appreciably from study to study, or from property to property, without the correspondent error changing significantly; i.e., large changes in ranking may be associated with small changes in the MUE. Oppositely, small changes in ranking may involve large differences in the MUEs. The readers are advised to take these aspects under consideration before choosing a density functional. More details on each study can be found in the original papers. From the analysis of Table 3, the development of the field of DFT is clearly visible. Today, several new density functionals are available, and new ones continue to appear, leading the accuracy of DFT in the determination of chemical properties to new levels.

B3LYP still remains a valid and particularly efficient alternative for the "average" quantum chemistry problem. It has marked an age and still dominates the field (see Figure 1). However, for some properties several new density functionals significantly outperform this popular hybrid functional (Table 3). The determination of barrier heights is one of such cases. The MUE associated with B3LYP in the determination of barrier heights is typically over 3 kcal/mol, with B3LYP demonstrating a marked tendency to underestimate this quantity. New functionals, such as BB1K are normally able to calculate barrier heights with an accuracy better than 1.5 kcal/mol. For other properties however, B3LYP is still able to compete in accuracy with the most sophisticated density functionals, and often at a fraction of the CPU time associated. Examples include geometry determination and the calculation of atomization energies and other thermochemical quantities for small organic molecules. There are, however, still some properties for which neither B3LYP nor the more sophisticated density functionals are able to give truly reliable results across a wide range of compounds. This is particularly true for nonbonded interactions, and most notably for weak and $\pi-\pi$-interactions, i.e., nonbonded interactions in which dispersion is the major source of attraction. Despite the progress in the field, the error in the determination of these quantities in comparison with the quantities themselves is normally too large to allow a reliable determination by standard DFT, even with most state-of-the-art density functionals.

Final Remarks

Globally, despite the general success of DFT in quantum chemistry, well portrayed in the overwhelming number of articles using this theory published over the last two decades, the application of DFT methodologies still holds some drawbacks. DFT is primarily a ground-state oriented method. Tricks enabling its application to excited states have been developed, albeit with a significant loss of accuracy and simplicity of

application. Hence, DFT cannot normally compete with semiempirical and post-Hartree−Fock methodologies in calculations involving excited states having the same symmetry as the ground state, and its application to degenerate states is also particularly troublesome.[116] Another important limitation of DFT concerns its nonvariational nature. In fact, DFT uses approximate functionals for the exchange and correlation terms. Hence, it is not variational and energy values below the true ground-state energy can be obtained, and the use of more complete basis sets does not necessarily lead to an improvement in accuracy. Weak interactions, as outlined above, are also a typical limitation of current density functionals, with DFT normally failing for van der Waals interactions.

New density functionals continue to appear, taking the performance of DFT to new and new levels of accuracy. B3LYP is still the most widely used functional (81% of publications in 2006) and will continue to be so over the next 3 or 4 years, but its long and almost undisputed reign seems to be approaching its final days. The general idea that has so deeply established, during the past decade, B3LYP as the functional of election for DFT calculations, the quantum chemistry's panacea, the functional to use "no-questions-asked", seems to be now well dead and buried. We are in an era of change. Several new density functionals have already been shown to significantly outdo B3LYP for several chemical properties, and new ones continue to appear. The difficulty will lie in choosing, from the plethora of new density functionals, the one to apply. None of the new density functionals has been shown to systematically overshadow all the others, and we predict that no density functional will succeed B3LYP as an unanimous number one choice. All have their strengths and weaknesses, but not all of them are known.

The selection of the functional to use will have to depend on the problem at hand, i.e., on both the property and type of system under study, and on the availability and computational expense associated. The user is now prompted to carefully weigh all these aspects before embarking in a new DFT study, or he will sooner or later have to take his chances with readers, wanting to know why he has chosen this functional instead of that one, why not that one, or why not the reader's favorite one, what would the results be had he used that other one instead, and so on. The only possible defense to some of these pungent questions is to be always on the lookout for new benchmarking studies, to test several density functionals against experimental data or higher-level methods on the specific system under consideration, and to ultimately redo all the calculations with more than one density functional just to be sure. This is becoming every day more a time of plurality of alternatives than that of a sheer domination by one single functional. The upcoming years will say.

References and Notes

(1) Jensen, F. *Introduction to Computational Chemistry*, 1st ed.; John Wiley & Sons: Chichester, England, 2004.

(2) Parr, R. G. *Annu. Rev. Phys. Chem.* **1983**, *34*, 631.

(3) Ziegler, T. *Chem. Rev.* **1991**, *91*, 651.

(4) Parr, R. G.; Yang, W. T. *Annu. Rev. Phys. Chem.* **1995**, *46*, 701.

(5) Gonze, X. *Phys. Rev. A* **1995**, *52*, 1096.

(6) Kohn, W.; Becke, A. D.; Parr, R. G. *J. Phys. Chem.* **1996**, *100*, 12974.

(7) Baerends, E. J.; Gritsenko, O. V. *J. Phys. Chem. A* **1997**, *101*, 5383.

(8) Chermette, H. *Coord. Chem. Rev.* **1998**, *180*, 699.

(9) Siegbahn, P. E. M.; Blomberg, M. R. A. *Annu. Rev. Phys. Chem.* **1999**, *50*, 221.

(10) Geerlings, P.; De Proft, F.; Langenaeker, W. *Chem. Rev.* **2003**, *103*, 1793.

(11) Burke, K.; Werschnik, J.; Gross, E. K. U. *J. Chem. Phys.* **2005**, *123*.

(12) Fermi, E. *Rend. Accad. Naz. Lincei* **1927**, *6*, 602.

(13) Thomas, L. H. *Proc. Cambridge Philos. Soc.* **1927**, *23*, 542.

(14) Slater, J. C. *Phys. Rev.* **1951**, *81*, 385.

(15) Hohenberg, P.; Kohn, W. *Phys. Rev. B* **1964**, *136*, 864.

(16) Kohn, W.; Sham, L. J. *Phys. Rev. A* **1965**, *140*, 1133.

(17) Dirac, P. A. M. *Proc. Cambridge Philos. Soc.* **1930**, *26*, 376.

(18) Weizsäcker, C. F. Z. *Phys.* **1935**, *36*, 431.

(19) Vosko, S. H.; Wilk, L.; Nusair, M. *Can. J. Phys.* **1980**, *58*, 1200.

(20) Ceperley, D. *Phys. Rev. B* **1978**, *18*, 3126.

(21) Ceperley, D. M.; Alder, B. J. *Phys. Rev. Lett.* **1980**, *45*, 566.

(22) Perdew, J. P.; Zunger, A. *Phys. Rev. B* **1981**, *23*, 5048.

(23) Becke, A. D. *J. Chem. Phys.* **1986**, *84*, 4524.

(24) Becke, A. D. *J. Chem. Phys.* **1992**, *96*, 2155.

(25) Becke, A. D. *J. Chem. Phys.* **1992**, *97*, 9173.

(26) Becke, A. D. *J. Chem. Phys.* **1993**, *98*, 5648.

(27) Becke, A. D. *J. Chem. Phys.* **1996**, *104*, 1040.

(28) Becke, A. D. *J. Chem. Phys.* **1997**, *107*, 8544.

(29) Becke, A. D. *Phys. Rev. A* **1988**, *38*, 3098.

(30) Perdew, J. P.; Wang, Y. *Phys. Rev. B* **1986**, *33*, 8800.

(31) Adamo, C.; Barone, V. *J. Chem. Phys.* **1998**, *108*, 664.

(32) Handy, N. C.; Cohen, A. J. *Mol. Phys.* **2001**, *99*, 403.

(33) Xu, X.; Goddard, W. A., III. *Proc. Natl. Acad. Sci. U.S.A.* **2004**, *101*, 2673.

(34) Kurth, S.; Perdew, J. P.; Blaha, P. *Int. J. Quantum Chem.* **1999**, *75*, 889.

(35) Wang, Y.; Perdew, J. P. *Phys. Rev. B* **1991**, *43*, 8911.

(36) Perdew, J. P. *Phys. Rev. Lett.* **1985**, *55*, 1665.

(37) Perdew, J. P. *Phys. Rev. B* **1986**, *33*, 8822.

(38) Perdew, J. P. Unified Theory of Exchange and Correlation Beyond the Local Density Approximation. In *Electronic Structure of Solids '91*; Ziesche, P., Eschig, H., Eds.; Akademie Verlag: Berlin, Germany, 1991; pp 11−20.

(39) Perdew, J. P.; Wang, Y. *Phys. Rev. B* **1992**, *45*, 13244.

(40) Perdew, J. P.; Burke, K.; Ernzerhof, M. *Phys. Rev. Lett.* **1996**, *77*, 3865.

(41) Langreth, D. C.; Perdew, J. P. *Phys. Rev. B* **1980**, *21*, 5469.

(42) Adamo, C.; Barone, V. *J. Chem. Phys.* **2002**, *116*, 5933.

(43) Becke, A. D. *J. Chem. Phys.* **1988**, *88*, 1053.

(44) Lee, C.; Yang, W.; Parr, R. G. *Phys. Rev. B* **1988**, *37*, 785.

(45) Colle, R.; Salvetti, D. *Theor. Chim. Acta* **1975**, *37*, 329.

(46) Langreth, D. C.; Mehl, M. J. *Phys. Rev. B* **1983**, *28*, 1809.

(47) Perdew, J. P.; Chevary, J. A.; Vosko, S. H.; Jackson, K. A.; Pederson, M. R.; Singh, D. J.; Fiolhais, C. *Phys. Rev. B* **1992**, *46*, 6671.

(48) Proynov, E. I.; Ruiz, E.; Vela, A.; Salahub, D. R. *Int. J. Quantum Chem.* **1995**, *29*, 61.

(49) Tao, J. M.; Perdew, J. P. *J. Chem. Phys.* **2005**, *122*, Art. No. 114102.

(50) Patton, D. C.; Pederson, M. R. *Phys. Rev. A* **1997**, *56*, 2495.

(51) Leung, T. C.; Chan, C. T.; Harmon, B. N. *Phys. Rev. B* **1991**, *44*, 2923.

(52) Engel, E.; Vosko, S. H. *Phys. Rev. B* **1994**, *50*, 10498.

(53) Barbiellini, B.; Moroni, E. G.; Jarlborg, T. *J. Phys. Condens. Matter* **1990**, *2*, 7597.

(54) Korling, M.; Haglund, J. *Phys. Rev. B* **1992**, *45*, 13293.

(55) Singh, D. J.; Ashkenazi, J. *Phys. Rev. B* **1992**, *46*, 11570.

(56) Dufek, P.; Blaha, P.; Schwarz, K. *Phys. Rev. B* **1994**, *50*, 7279.

(57) Khein, A.; Singh, D. J.; Umrigar, C. J. *Phys. Rev. B* **1995**, *51*, 4105.

(58) Kutzler, F. W.; Painter, G. S. *Phys. Rev. B* **1991**, *43*, 6865.

(59) Krieger, J. B.; Chen, J.; Iafrate, G. J.; Savin, A. *Electron Correl. Mater. Prop.* **1999**, 463.

(60) Tao, J.; Perdew, J. P.; Staroverov, V. N.; Scuseria, G. E. *Phys. Rev. Lett.* **2003**, *91*, Art. No. 146401.

(61) Van Voorhis, T.; Scuseria, G. E. *J. Chem. Phys.* **1998**, *109*, 400.

(62) Becke, A. D. *J. Chem. Phys.* **1993**, *98*, 1372.

(63) Hamprecht, F. A.; Cohen, A. J.; Tozer, D. J.; Handy, N. C. *J. Chem. Phys.* **1998**, *109*, 6264.

(64) Schmider, H. L.; Becke, A. D. *J. Chem. Phys.* **1998**, *108*, 9624.

(65) Lynch, B. J.; Fast, P. L.; Harris, M.; Truhlar, D. G. *J. Phys. Chem. A* **2000**, *104*, 4811.

(66) Lynch, B. J.; Zhao, Y.; Truhlar, D. G. *J. Phys. Chem. A* **2003**, *107*, 1384.

(67) Schultz, N. E.; Zhao, Y.; Truhlar, D. G. *J. Phys. Chem. A* **2005**, *109*, 11127.

(68) Zhao, Y.; Gonzalez-Garcia, N.; Truhlar, D. G. *J. Phys. Chem. A* **2005**, *109*, 2012.

(69) Zhao, Y.; Lynch, B. J.; Truhlar, D. G. *J. Phys. Chem. A* **2004**, *108*, 2715.

(70) Zhao, Y.; Truhlar, D. G. *J. Phys. Chem. A* **2004**, *108*, 6908.

(71) Zhao, Y.; Truhlar, D. G. *J. Chem. Theory Comput.* **2005**, *1*, 415.

(72) Zhao, Y.; Truhlar, D. G. *Phys. Chem. Chem. Phys.* **2005**, *7*, 2701.

(73) Keal, T. W.; Tozer, D. J. *J. Chem. Phys.* **2005**, *123*, Art. No. 121103.

(74) Boese, A. D.; Martin, J. M. L. *J. Chem. Phys.* **2004**, *121*, 3405.

(75) Gill, P. M. W. *Mol. Phys.* **1996**, *89*, 433.

(76) Zhao, Y.; Schultz, N. E.; Truhlar, D. G. *J. Chem. Phys.* **2005**, *123*, Art. No. 161103.

(77) Zhao, Y.; Schultz, N. E.; Truhlar, D. G. *J. Chem. Theory Comput.* **2006**, *2*, 364.

(78) Zhao, Y.; Truhlar, D. G. *J. Phys. Chem. A* **2004**, *108*, 6908.

(79) Hoe, W. M.; Cohen, A. J.; Handy, N. C. *Chem. Phys. Lett.* **2001**, *341*, 319.

(80) Zhao, Y.; Truhlar, D. G. *J. Phys. Chem. A* **2005**, *109*, 5656.

(81) Slater, J. C. *The Self-Consistent Field for Molecular and Solids*; McGraw-Hill: New York, 1974; Vol. 4.

(82) Perdew, J. P.; Schmidt, K. Jacob's ladder of density functional approximations for the exchange−correlation energy. In *Density Functional Theory and Its Applications to Materials*; Van Doren, V. E., Van Alseoy, K., Geerlings, P., Eds.; AIP Press: New York, 2001.

(83) Johnson, B. G.; Gill, P. M. W.; Pople, J. A. *J. Chem. Phys.* **1992**, *97*, 7846.

(84) Johnson, B. G.; Gill, P. M. W.; Pople, J. A. *J. Chem. Phys.* **1993**, *98*, 5612.

(85) Bauschlicher, C. W. *Chem. Phys. Lett.* **1995**, *246*, 40.

(86) Scheiner, A. C.; Baker, J.; Andzelm, J. W. *J. Comput. Chem.* **1997**, *18*, 775.

(87) Neugebauer, A.; Hafelinger, G. *J. Mol. Struct. (THEOCHEM)* **2002**, *578*, 229.

(88) Neugebauer, A.; Hafelinger, G. *J. Mol. Struct. (THEOCHEM)* **2002**, *585*, 35.

(89) Lynch, B. J.; Truhlar, D. G. *J. Phys. Chem. A* **2002**, *106*, 842.

(90) Mole, S. J.; Zhou, X. F.; Liu, R. F. *J. Phys. Chem.* **1996**, *100*, 14665.

(91) Curtiss, L. A.; Raghavachari, K.; Redfern, P. C.; Pople, J. A. *J. Chem. Phys.* **1997**, *106*, 1063.

(92) Curtiss, L. A.; Redfern, P. C.; Raghavachari, K.; Pople, J. A. *J. Chem. Phys.* **1998**, *109*, 42.

(93) Ernzerhof, M.; Scuseria, G. E. *J. Chem. Phys.* **1999**, *110*, 5029.

(94) Rabuck, A. D.; Scuseria, G. E. *Chem. Phys. Lett.* **1999**, *309*, 450.

(95) Curtiss, L. A.; Raghavachari, K.; Redfern, P. C.; Pople, J. A. *J. Chem. Phys.* **2000**, *112*, 7374.

(96) Curtiss, L. A.; Redfern, P. C.; Rassolov, V.; Kedziora, G.; Pople, J. A. *J. Chem. Phys.* **2001**, *114*, 9287.

(97) Hobza, P.; Sponer, J.; Reschel, T. *J. Comput. Chem.* **1995**, *16*, 1315.

(98) Paizs, B.; Suhai, S. *J. Comput. Chem.* **1998**, *19*, 575.

(99) Halkier, A.; Klopper, W.; Helgaker, T.; Jorgensen, P.; Taylor, P. R. *J. Chem. Phys.* **1999**, *111*, 9157.

(100) Tuma, C.; Boese, A. D.; Handy, N. C. *Phys. Chem. Chem. Phys.* **1999**, *1*, 3939.

(101) Rabuck, A. D.; Scuseria, G. E. *Theor. Chem. Acc.* **2000**, *104*, 439.

(102) Rappe, A. K.; Bernstein, E. R. *J. Phys. Chem. A* **2000**, *104*, 6117.

(103) Tsuzuki, S.; Luthi, H. P. *J. Chem. Phys.* **2001**, *114*, 3949.

(104) Stamant, A.; Cornell, W. D.; Kollman, P. A. *J. Comput. Chem.* **1995**, *16*, 1483.

(105) Wang, N. X.; Wilson, A. K. *J. Chem. Phys.* **2004**, *121*, 7632.

(106) Riley, K. E.; Brothers, E. N.; Ayers, K. B.; Merz, K. M. *J. Chem. Theory Comput.* **2005**, *1*, 546.

(107) Schultz, N. E.; Zhao, Y.; Truhlar, D. G. *J. Phys. Chem. A* **2005**, *109*, 4388.

(108) Riley, K. E.; Op't Holt, B. T.; Merz, K. M., Jr. *J. Chem. Theory Comput.* **2007**, *3*, 407.

(109) Zhao, Y.; Pu, J.; Benjamin, J. L.; Truhlar, D. G. *Phys. Chem. Chem. Phys.* **2004**, *6*, 673.

(110) Zhao, Y.; Truhlar, D. G. *J. Phys. Chem. A* **2006**, *124*, 224105.

(111) Brothers, E. N.; Merz, K. M. *J. Phys. Chem A* **2004**, *108*, 2904.

(112) Curtiss, L. A.; Redfern, P. C.; Raghavachari, K. *J. Chem. Phys.* **2005**, *123*, Art. No. 124107.

(113) Zhao, Y.; Truhlar, D. G. *J. Phys. Chem. A* **2006**, *110*, 10478.

(114) Zhao, Y.; Tishchenko, O.; Truhlar, D. G. *J. Phys. Chem. B* **2005**, *109*, 19046.

(115) Zhao, Y.; Truhlar, D. G. *J. Phys. Chem. A* **2006**, *110*, 5121.

(116) Bersuker, I. B. *J. Comput. Chem.* **1997**, *18*, 260.